On Stability and Tuning of Neural Oscillators: Application to Rhythmic Control of a Humanoid Robot

Artur M. Arsenio
Computer Science and Artificial Intelligence Laboratory
Massachusetts Institute of Technology
Cambridge, MA 02139
E-mail: arsenio@csail.mit.edu

Abstract— **Neural oscillators offer a natural tool for exploiting and adapting to the dynamics of the controlled system. The capability of entraining the frequency of the input signal or resonance modes of dynamical systems have been increasingly used in robotics' mechanisms, to accomplish complex tasks. However, the application of Matsuoka neural oscillators as controllers requires the knowledge of the range of values for the parameters for which the system oscillates, and the warranty of stability. Thus, this paper studies in depth the stability and tuning of Matsuoka neural oscillators, and presents a careful analysis of its behavior on the time-domain. The method is applied on a Humanoid Robot for playing musical instruments.**

I. INTRODUCTION

The stability analysis of Matsuoka neural oscillators for a determined range of values will be carried out using tools from contraction analysis, [7], and invariant set theory (La Salle Theorem, [9]). To this end, the oscillator analysis in the time domain is performed separately for each of the regions in which the dynamics is linear.

Certain reflexes, such as some spinal reflexes, also consist of Rhythmic movements. For example, rhythmic scratching occurs after the animal having moved his limb to the starting posture. Even in animals with the cervical cord damaged at the cervical level, the reflexes still occur, [6]. Although these reflexes do not require input from higher-order cortical centers, they depend on feedback from sensors, since properties of the reflex depend both on duration and intensity of the stimulus, [6]. Another important activity generated by innate spinal circuits is walking. Indeed, Central Pattern Generators located in the spinal cord, generate coordinated rhythmic patterns for the contraction of the several muscle groups involved in the movement.

These neural circuits are often modelled using a half-center model, consisting of motor neurons having mutually inhibitory synapses. Networks of Matsuoka neural oscillator may be used to model complex neural circuits, [11]. Furthermore, there is also biological evidence that humans exploit the dynamics of their body (e.g., arms) to accomplish a desired task, and this property is also fully exploited by such networks.

The Matsuoka neural oscillator consists of two neurons inhibiting each other mutually. The nonlinear dynamics of the neural oscillator follows the equations presented in Figure 1. Each neuron have two states variables, c is a positive tonic input, τ_1 and τ_2 are positive time constants, β, γ (usually both positives) and $k_i \geq 0$ are weights, and g_i is an external input to the oscillator. There are two types of nonlinearities: $n(u) = n^+(u) = max(u, 0)$, and $n^-(u) = -min(u, 0) = max(-u, 0)$, with u being the nonlinearity input.
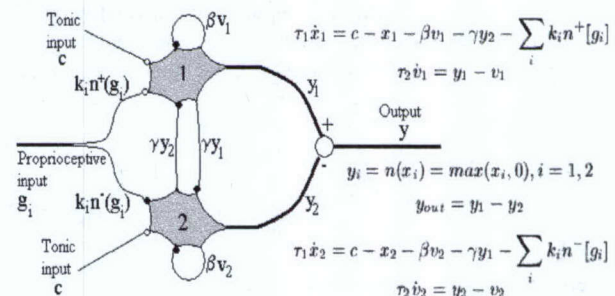

Fig. 1. Matsuoka neural oscillator, composed by two inhibiting neurons.

Previous work provided an extensive analysis of these neural oscillators on the frequency domain [2], [1]. This paper presents a detailed analysis on the time-domain using several appropriate mathematical tools. It will then describe an experiment on the Humanoid robot Cog showing the benefits of such analysis.

II. TIME-DOMAIN PARAMETER ANALYSIS

Matsuoka neural oscillators nonlinearities are all linear by parts, [13]. For example, the $max(x, 0)$ nonlinearity has a unity gain when the input is non-negative and zero otherwise. All the nonlinearities of this oscillator may thus be decomposed into regions of operation, and analyzed with linear tools in that regions. Since the oscillator nonlinearities are all continuous, the system is well defined at the boundary of these regions (although the derivatives are not). In this paper, it is presented a time domain analysis for a piece-linear model of the dynamical system, which will bring more insight to variation of oscillator's oscillations with parameters,

and to stability issues. The time-domain description allows a better comprehension of the neural oscillator, being possible the determination of the range of values for which the neural oscillator converges: to a stable equilibrium point, to a stable limit cycle or to a stable limit set. A similar time-domain analysis for the study of the parameters was presented by Matsuoka, [8], using a mathematical formalism, instead of considering the neural oscillator as a piece-wise linear system, as proposed in [13]. When converging to a limit set, some of the internal state variables may diverge along some eigen-directions, but the others converge to zero, implying a volume contraction in the state-space, as described in Section 3.1 using Volume Contraction Analysis.

A. Free Vibrations

The piece-linear dynamic equations of one oscillator for free vibrations, i.e., without an applied input, are,

$$
\begin{bmatrix} \dot{x}_1 \\ \dot{v}_1 \\ \dot{x}_2 \\ \dot{v}_2 \end{bmatrix} = \begin{bmatrix} -\frac{1}{\tau_1} & -\frac{\beta}{\tau_1} & -\frac{\gamma}{\tau_1}u_2^x & 0 \\ \frac{1}{\tau_2}u_1^x & -\frac{1}{\tau_2} & 0 & 0 \\ -\frac{\gamma}{\tau_1}u_1^x & 0 & -\frac{1}{\tau_1} & -\frac{\beta}{\tau_1} \\ 0 & 0 & \frac{1}{\tau_2}u_2^x & -\frac{1}{\tau_2} \end{bmatrix} \begin{bmatrix} x_1 \\ v_1 \\ x_2 \\ v_2 \end{bmatrix}
$$

$$
+ \begin{bmatrix} \frac{c}{\tau_1} & 0 & \frac{c}{\tau_1} & 0 \end{bmatrix}^T \iff \dot{X} = A_{ij}X + B \tag{1}
$$

where u_i^x, for i=1,2, is the unit input function relative to x_i, i.e., it cancels for negative values and is equal to unity for positive values. To check for stability of the equilibrium points, results:

$$
\begin{vmatrix} \lambda + \frac{1}{\tau_1} & \frac{\beta}{\tau_1} & \frac{\gamma}{\tau_1}u_2^x & 0 \\ \frac{1}{\tau_2}u_1^x & \lambda + \frac{1}{\tau_2} & 0 & 0 \\ \frac{\gamma}{\tau_1}u_1^x & 0 & \lambda + \frac{1}{\tau_1} & \frac{\beta}{\tau_1} \\ 0 & 0 & -\frac{1}{\tau_2}u_2^x & \lambda + \frac{1}{\tau_2} \end{vmatrix} = 0 \tag{2}
$$

Lets consider the four possible cases:

- $u_1^x = 1 \; and \; u_2^x = 1$

From (1), the equilibrium point is,

$$
x_1^* = x_2^* = v_1^* = v_2^* = \frac{c}{\beta+\gamma+1} \tag{3}
$$

For $c \geq 0$ and $\beta + \gamma \geq -1$ the equilibrium point belongs to the region of the state space considered, and therefore this is an equilibrium point for all the system. If c and $\beta+\gamma+1$ have opposite signs, then the equilibrium is located in the third quadrant and it is not an equilibrium point of the overall system (these points will be thereafter called *virtual equilibrium points*). The stability of the equilibrium point is determined by (2), being the eigenvalues given by (4),

$$
\lambda_{1,2} = -\frac{1}{2}\epsilon_1 \pm \frac{1}{2}\sqrt{\epsilon_1^2 - 4\frac{\beta-\gamma+1}{\tau_1\tau_2}}
$$
$$
\lambda_{3,4} = -\frac{1}{2}\epsilon_2 \pm \frac{1}{2}\sqrt{\epsilon_2^2 - 4\frac{\beta+\gamma+1}{\tau_1\tau_2}}
\tag{4}
$$

where $\epsilon_1 = \frac{1-\gamma}{\tau_1} + \frac{1}{\tau_2}$ and $\epsilon_2 = \frac{1+\gamma}{\tau_1} + \frac{1}{\tau_2}$. The corresponding eigenvectors are,

$$
\begin{aligned} v_{1,2} = [\alpha_{1,2} \; 1 \; \alpha_{1,2} \; 1]^T & \quad \alpha_{1,2} = \tau_2\lambda_{1,2} + 1 \\ v_{3,4} = [-\alpha_{3,4} \; -1 \; \alpha_{3,4} \; 1]^T & \quad \alpha_{3,4} = \tau_2\lambda_{3,4} + 1 \end{aligned} \tag{5}
$$

The first two eigenvalues are in the left half of the complex plane if $\beta > \gamma - 1$ and $\gamma < 1 + \frac{\tau_1}{\tau_2}$, and the other two if $\beta > -\gamma-1$ and $\gamma > -1-\frac{\tau_1}{\tau_2}$. Therefore, this point is asymptotically stable if $\beta > max(-\gamma - 1, \gamma - 1)$ and $-1 - \frac{\tau_1}{\tau_2} < \gamma < +1 + \frac{\tau_1}{\tau_2}$. The point would have all manifolds unstable if $\beta < min(-\gamma - 1, \gamma - 1)$ and $+1 + \frac{\tau_1}{\tau_2} < \gamma < -1 - \frac{\tau_1}{\tau_2}$. Since the time constants τ_1 and τ_2 are both positive, this last condition is impossible. Therefore the system' stability depends only on the values of γ and β, and may correspond to a stable or a saddle equilibrium point. A saddle point with two unstable and two stable manifolds (one of the essential conditions for free oscillations for this oscillator) if:

$$
\beta > max(-\gamma - 1, \gamma - 1)
$$
$$
\gamma < -1 - \frac{\tau_1}{\tau_2} \; or \; \gamma > +1 + \frac{\tau_1}{\tau_2}.
$$

For $\tau_1 = 0.1$, $\tau_2 = 0.2$, $\gamma = \beta = 2$, the equilibrium point is a four dimensional saddle point, with two directions converging and the other two diverging, as shown in Figure 2-b.
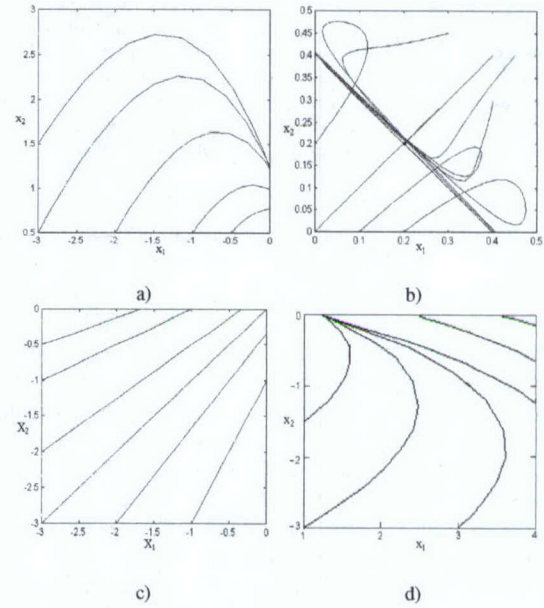

a)

b)

c)

d)

Fig. 2. Plot of the neural oscillator by linear parts: a) $x_1 < 0$, $x_2 \geq 0$ b) $x_1, x_2 \geq 0$ c) $x_1, x_2 < 0$ d) $x_1 \geq 0$, $x_2 < 0$. The parameters used were: $\tau_1 = 0.1$, $\tau_2 = 0.2$, $\beta = \gamma = 2$, and $c = 1$.

- $u_1^x = 1 \; and \; u_2^x = 0$

The equilibrium point in this case is:

$$
x_1^* = v_1^* = \frac{c}{\beta+1}, \quad x_2^* = c\frac{\beta-\gamma+1}{\beta+1}, \quad v_2^* = 0 \tag{6}
$$

The stability of the equilibrium point is determined by the eigenvalues:

$$
\lambda_1 = -\frac{1}{\tau_1}, \quad \lambda_2 = -\frac{1}{\tau_2}
$$
$$
\lambda_{3,4} = -\frac{\left(\frac{1}{\tau_1}+\frac{1}{\tau_2}\right)}{2} \pm \frac{\sqrt{\left(\frac{1}{\tau_1}+\frac{1}{\tau_2}\right)^2 - 4\frac{\beta+1}{\tau_1\tau_2}}}{2} \tag{7}
$$

and the corresponding eigenvectors,

$$v_1 = \begin{bmatrix} 0 & 0 & -\frac{\beta\tau_2}{\tau_2-\tau_1} & 1 \end{bmatrix}^T$$
$$v_2 = \begin{bmatrix} 0 & 0 & 1 & 0 \end{bmatrix}^T \tag{8}$$
$$v_{3,4} = \begin{bmatrix} -\frac{\tau_1\lambda)3,4+1}{\gamma} & \alpha_{3,4} & 1 & 0 \end{bmatrix}^T$$

$$\alpha_{3,4} = \frac{1}{\gamma\beta\tau_2}\left(-\tau_1^2\lambda_{3,4} - \frac{3\tau_1}{2} + \frac{\tau_2}{2} \pm \frac{\sqrt{(\tau_1-\tau_2)^2 - 4\tau_1\tau_2\beta}}{2} - \tau_1\beta\right)$$

This equilibrium is stable unless $\beta < -1$, value for which it is unstable. However, only if β and γ are within a certain range of values the eq. is on the fourth quadrant. For other values, this becomes a *virtual* equilibrium point, since it is not an equilibrium point for the overall system. For $\tau_1 = 0.1$, $\tau_2 = 0.2$, $\gamma = \beta = 2$, the equilibrium point is stable and coincident with the equilibrium point for $x_1 \geq 0$ and $x_2 \geq 0$, as illustrated in Figure 2-d.

- $u_1^x = 0$ and $u_2^x = 1$

Since the equations are symmetric, this case is similar to the previous, and thus the same analysis holds interchanging x_1 and x_2. The eigenvalues and eigenvectors are the same, and the state-space trajectories for this region are illustrated in Figure 2-a.

- $u_1^x = 0$ and $u_2^x = 0$

The equilibrium point of the piece-linear dynamic equations is

$$x_1^* = x_2^* = c, \quad v_1^* = v_2^* = 0 \tag{9}$$

The stability of this equilibrium point is determined by the eigenvalues,

$$\lambda_{1,2} = -\frac{1}{\tau_1}, \quad \lambda_{3,4} = -\frac{1}{\tau_2} \tag{10}$$

and the associated eigenvectors are,

$$v_1 = \begin{bmatrix} 1 & 0 & 0 & 0 \end{bmatrix}^T, \qquad v_2 = \begin{bmatrix} 0 & 0 & 1 & 0 \end{bmatrix}^T$$
$$v_3 = \begin{bmatrix} \frac{\beta\tau_2}{\tau_1-\tau_2} & 1 & 0 & 0 \end{bmatrix}^T, \quad v_4 = \begin{bmatrix} 0 & 0 & \frac{\beta\tau_2}{\tau_1-\tau_2} & 1 \end{bmatrix}^T \tag{11}$$

This equilibrium is always stable. However, only a negative tonic would locate the equilibrium on the third quadrant. Therefore, this is a *virtual* equilibrium point, as illustrated in Figure 2-c.

From the exposed, for a zero tonic input (which is always non-negative), the equilibrium point is $(0,0,0,0)$, and therefore all the trajectories will converge to this equilibrium point. Indeed, even if the initial conditions are in the first quadrant, as soon as x_1 or x_2 changes sign, the trajectory will converge asymptotically to the equilibrium, and the system does not oscillate. Therefore, from the previous conditions, for free oscillations $k = \frac{\tau_2}{\tau_1}$, β and γ must satisfy (12).

$$\beta > max(-\gamma-1, \gamma-1, -1)$$
$$\gamma < -1 - 1/k \text{ or } \gamma > +1 + 1/k \tag{12}$$

However, for $\gamma < 0$, $x_1 = x_2$, i.e., the states oscillate on phase, and therefore the output is zero. Thus, (12) is simplified to (13), which is the same result obtained by Matsuoka, [8], using a different methodology.

$$\beta > \gamma - 1, \quad \gamma > +1 + 1/k \tag{13}$$

B. Forced Vibrations

Generally, the oscillator has a non-zero input g. The main changes on the previous analysis is that now there are two more conditions to be tested, $g > 0$ and $g < 0$, which implies that the system becomes piece-wise linear in eight regions. A constant input $g = D > 0$ (if $D < 0$, the analysis is the same, interchanging indices 1 and 2) is going to change the location of the equilibrium point as follows:

- $x_1 \geq 0$ and $x_2 \geq 0$
$$x_1^* = v_1^* = \frac{c}{\beta+\gamma+1} - \frac{1+\beta}{(1+\beta)^2-\gamma^2}D$$
$$x_2^* = v_2^* = \frac{c}{\beta+\gamma+1} + \frac{\gamma}{(1+\beta)^2-\gamma^2}D$$
- $x_1 \geq 0$ and $x_2 < 0$
$$x_1^* = v_1^* = \frac{c-D}{\beta+1}, \quad x_2^* = \frac{c(\beta+1-\gamma)+\gamma D}{\beta+1}, \quad v_2^* = 0$$
- $x_1 < 0$ and $x_2 \geq 0$
$$x_2^* = v_2^* = \frac{c}{\beta+1}, \quad x_1^* = c\frac{\beta+1-\gamma}{\beta+1} - D, \quad v_1^* = 0$$
- $x_1 < 0$ and $x_2 < 0$
$$x_1^* = c - D, \quad x_2^* = c, \quad v_1^* = v_2^* = 0$$

The system's oscillation depends on having three *virtual* attractors in the first quadrant and one real repulsor there. For a constant positive input $D < c\frac{\beta+1-\gamma}{\beta+1}$, or for a constant negative input $D < -c\frac{\beta+1-\gamma}{\gamma}$, the stable *virtual* equilibrium point in region $x_1 < 0$ and $x_2 \geq 0$ becomes a true one, while the unstable equilibrium changes quadrant and therefore becomes *virtual*. Therefore, the system converges now to the stable equilibrium and therefore there are no oscillations, as shown in Figure 3-b. Figure 3-a shows the state-space for free vibrations, for an experiment using the same parameters as in Figure 2, [13].
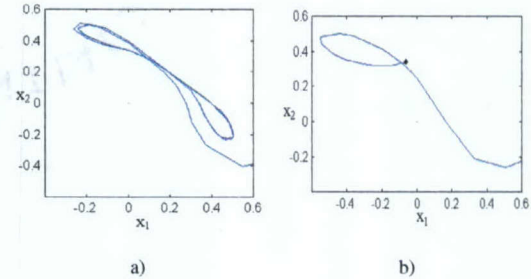

a)

b)

Fig. 3. a) Simulation for free vibrations, using the MATLAB Simulink Control Box. b) Simulation for a constant input. The neural oscillator does not oscillates, and converges to the stable equilibrium point.

C. Transients

The Matsuoka neural oscillator is very robust to perturbations, [13]. The oscillator usually converges very fast, being often one time period enough for the transient to disappear. However, the duration of the transient depends on the eigenvalues of the dynamics at each region. By tuning γ, β, τ_1 and τ_2, it is possible to design the system with very fast transients and with a desired frequency bandwidth.

When the amplitude of the input signal decreases, for a certain range of input amplitude value the oscillator output is oscillating at two frequencies, corresponding to the input frequency and to the oscillator's free vibration frequency $w_{n_{osc}}$. If the input amplitude is increased/decreased from these range of values, the oscillator spectrum will be concentrated on only one frequency: input frequency w or $w_{n_{osc}}$, respectively. This may occur after a transient in which the oscillator output spectrum power is concentrated on two frequencies, as shown in Figure 4-a.
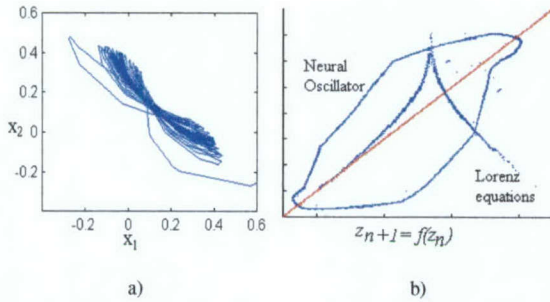

a) b)

Fig. 4. a) Transients in oscillations. The oscillator initially oscillates at low frequency, but converges slowly to a higher frequency limit cycle. b) Lorenz maps for the neural oscillator and Lorenz equations.

Figure 4-b shows the *Lorenz map*, [10], for the neural oscillator versus Lorenz equations [10]. In the graph, z_n is the local maximum of $z(t)$ (Lorenz equations) or of the oscillator output y_{osc}. The function $z_{n+1} = f(z_n)$ is called the Lorenz map. If $|f'(z)| > 1$ everywhere, then if any limit cycle exist, they are necessarily unstable. Thus, observing Figure 4-b, contrary to Lorenz equations, the neural oscillator does not present Chaotic behavior during the transients.

III. CONTRACTION ANALYSIS

Contraction analysis, [7], is a method inspired from fluid mechanics and differential theory, that analyzes convergence between two neighboring trajectories by considering the local flow at a given point. Following the definition presented in [7], given $\dot{x} = f(x,t)$, the region of the state-space where the Jacobian $\partial f / \partial x$ is uniformly negative definite,

$$\exists \beta > 0, \forall t \geq 0, \frac{1}{2}\left(\frac{\partial f}{\partial x} + \frac{\partial f^T}{\partial x}\right) \leq -\alpha I < 0 \quad (14)$$

is denominated a contraction region. However, partial derivatives do not exist on regions boundaries. Therefore, contraction analysis is applied to each linear region of the neural oscillator.

Applying (14) to (1), for each of the four piece-wise linear regions, results that the dynamics do not contract in any of these regions (indeed, there is at least one positive eigenvalue of the matrix defined by (14), in each linear region). This is because, for the parameters necessary for oscillations, given by (13), the dynamics in any of the three quadrants where $x_1 < 0$ or $x_2 < 0$ (or both), converges to a *virtual* stable equilibrium. Thus, these regions are not contracting – the *virtual* equilibrium points are not contained in these regions. For both $x_1, x_2 \geq 0$, the saddle equilibrium contains two unstable manifolds and two stable. Since the states have to transverse this region in both directions (see Figure 3-a), there is no trajectory to which all points converge.

A. Volume Contraction

The Matsuoka neural oscillator is dissipative, which means that volumes defined by the state space variables contract in time, although not all the states contract, as just referred. Lets select an arbitrary surface $S(t)$ of volume $V(t)$ in phase space, [10]. Considering f the instantaneous velocity of points on S (the initial conditions for trajectories), and n the outward normal on S, in time dt the volume expands $(fndt)dA$, and thus $\dot{V} = \int_S fndA$. Using the divergence theorem, results $\dot{V} = \int_V \nabla f dV$. Lets consider first the oscillator uncoupled, as described by (1):

$$\nabla \dot{f} = \frac{\partial}{\partial x_1} 1/\tau_1(c - x_1 - \beta v_1 - \gamma max(x_2, 0) - \sum_i k_i n^+(u_i))$$
$$+ \frac{\partial}{\partial v_1} 1/\tau_2(-\beta v_1 + max(x_1, 0)) +$$
$$\frac{\partial}{\partial x_2} 1/\tau_1(c - x_2 - \beta v_2 - \gamma max(x_1, 0) - \sum_i k_i n^-(u_i))$$
$$+ \frac{\partial}{\partial v_2} 1/\tau_2(-\beta v_2 + max(x_2, 0)) = -2/tau_1 - 2/tau_2 < 0$$

Therefore, since the divergence is constant, $\dot{V} = -2(1/\tau_1 + 1/\tau_2)V$. Thus, volumes in phase space shrink exponentially fast to a limiting set of zero volume, [10], and the rate of convergence only depends on the positive time constants τ_1 and τ_2.

For an oscillator coupled to a 2nd order system, the state space is now six-dimensional, being the two additional states θ_1 and θ_2, such that
$$\dot{\theta}_1 = \theta_2, \quad \dot{\theta}_2 = -k/m\theta_1 - b/m\theta_2 + k/m[y_1 - y_2]$$
resulting $\nabla f = -2/\tau_1 - 2/\tau_2 - b/m$, which is negative, since both the mass and the damping are positive. Therefore, volume contraction occurs. Since the Poincare-Bendixon theorem does not applies for systems with more than two dimensions, contraction analysis is a useful tool to infer volume convergence, and therefore contraction to a limit set.

Considering a multivariable input multivariable output (MIMO) closed-loop system consisting of two oscillators (with only one input for each oscillator), connected to a stable 4th order system,

$$\dot{\phi}_1 = \phi_2$$
$$\dot{\phi}_2 = \frac{1}{m_1}\left(-c_1\phi_2 - (k_1 + k_T)\phi_1 + k_2\phi_3 + k_1(y_1^1 - y_2^1)\right)$$
$$\dot{\phi}_3 = \phi_4$$
$$\dot{\phi}_4 = \frac{1}{m_2}\left(-c_2\phi_4 - (k_2 + k_T)\phi_3 + k_1\phi_1 + k_2(y_1^2 - y_2^2)\right)$$

results $\nabla f = -4/\tau_1 - 4/\tau_2 - c_1/m_1 - c_2/m_2 < 0$. Therefore, the volume of the MIMO close-loop system also contracts to a limit set. Since the volume contraction occurs $\forall \beta, \gamma$, even for unstable oscillations the volume still contracts. Indeed, there are eigenvectors in this 4th dimensional space along which the state converges to zero, and faster than the eigendirections along which the state may diverge.

IV. STABILITY ANALYSIS ON A PIECE-WISE LINEAR SYSTEM

Lets first investigate the operation of the neural oscillator in the 1st state-space quadrant. As described by (5), there are two eigenvectors $(v_{1,2})$ in which the 1st and 3rd elements are equal, as well as the 2nd and the 4th, and other two eigenvectors $(v_{3,4})$ in which the 1st and 3rd elements are symmetric, as well as the 2nd and the 4th elements. If there is an invariant set on this region, it must occur along $v_{3,4}$, since oscillations do not occur along $v_{1,2}$, because the states along these eigen-directions would oscillate in phase. Indeed, there are no invariant sets along $v_{1,2}$, which are the stable manifolds of the saddle point. Considering directions along $v_{3,4}$, and constrained to the fact that the saddle equilibrium point given by (3) is a solution in the state space, lets consider the set $S_1 \cap S_2$,

$$S_1 = \left\{ x_1 \geq 0, x_2 \geq 0 : x_1 + x_2 = \frac{2c}{\beta+1+\gamma} \right\}$$
$$S_2 = \left\{ v_1, v_2 : v_1 + v_2 = \frac{2c}{\beta+1+\gamma} \right\}$$

and apply to this set the local invariant set theorem (or La Salle theorem), [9]. This set is invariant for the dynamic system given by (1), in $\Omega_l = \{x_1 \geq 0, x_2 \geq 0\}$, if every system trajectory which starts from a point in this set remains in this set for all future time, [9]. For a proof, lets determine $\frac{\partial S_i}{\partial t}$, for i=1,2:

$$\dot{S_1} = \frac{1+\gamma}{-\tau_1}\left(x_1 + x_2 - \frac{2c}{\beta+1+\gamma} \right) - \frac{\beta}{\tau_1}\left(v_1 + v_2 - \frac{2c}{\beta+1+\gamma} \right)$$

$$\dot{S_2} = \frac{1}{\tau_2}\left[x_1 + x_2 - \frac{2c}{\beta+1+\gamma} - \left(v_1 + v_2 - \frac{2c}{\beta+1+\gamma} \right) \right]$$

Writing the equations in matrix notation, (15), it is easily concluded that the derivative is zero on the set. Thus, $S_1 \cap S_2$ is an invariant set.

$$\begin{bmatrix} \dot{S_1} \\ \dot{S_2} \end{bmatrix} = \begin{bmatrix} -\frac{1+\gamma}{\tau_1} & -\frac{\beta}{\tau_1} \\ \frac{1}{\tau_2} & -\frac{1}{\tau_2} \end{bmatrix} \begin{bmatrix} S_1 \\ S_2 \end{bmatrix} = Q \begin{bmatrix} S_1 \\ S_2 \end{bmatrix} \qquad (15)$$

Is this invariant set attractive? Lets consider a Lyapunov function (which represents a measure of the *distance* to the invariant set, [9]) and its time derivative,

$$V = \frac{1}{2}(S_1^2 + S_2^2)$$

$$\dot{V} = S_1\dot{S_1} + S_2\dot{S_2} = \begin{bmatrix} S_1 & S_2 \end{bmatrix} Q \begin{bmatrix} S_1 \\ S_2 \end{bmatrix}.$$

The matrix Q is negative definite for β and γ satisfying (13), since all eigenvalues of Q are negative for $\beta > -1 - \gamma$ and

$\gamma > -1 - 1/k$ (which once more demonstrates that oscillations are impossible for $\gamma < 0$, or $x_1 = x_2$). Thus, $\frac{\partial V}{\partial t}$ is zero only on the invariant set, and thus it is negative semi-definite. Therefore, applying the local invariant set theorem, [9], results that every solution in Ω_l tend to this invariant set as $t \rightarrow \infty$.

Matsuoka proofed in [8] that the output of the neural oscillator is bounded without any input. Williamson, in [13], extends the analysis for bounded inputs, and also demonstrates that for oscillators connected to LTI dynamic systems, the close-loop system variables are bounded. The output boundness, the existence of only unstable fixed points (for a certain range of the parameters), and the uniqueness of the solutions, by checking the Lipschitz condition, [13] (since the oscillator is linear by parts, it is locally Lipschitz in each linear region, [13]), imply that the oscillator has oscillatory solutions (not necessarily periodic), [13]. Furthermore, Williamson, using a method suggested in [5] based on the linearized *Poincaré map*, [10], also showed the local stability of a candidate limit cycle, by imposing conditions for the *Floquet multipliers*, [10].

The *Poincaré* map maps the n dimensional system $\dot{x} = f(x,t)$ into the $n-1$ discrete system $x_{k+1} = p(x_k)$, by intersecting the flow with a $n-1$ dimensional hypersurface transverse to the flow, [10]. Thus, it is possible to translate the problem of close orbits to one of fixed points of a mapping, as shown in Figure 5.
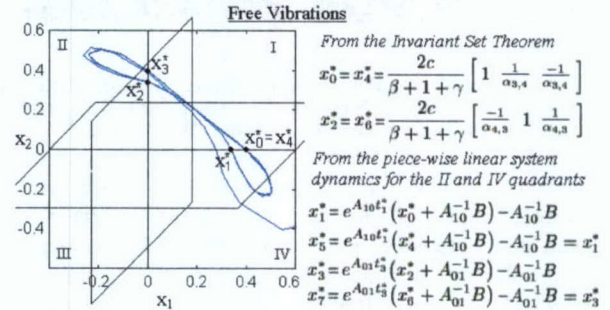

Fig. 5. Two surface sections transverse the flow of the neural oscillator at $x_1 = 0$ and at $x_2 = 0$.

V. APPLICATION TO OSCILLATORY CONTROL OF A HUMANOID ROBOT

The work here presented is part of the humanoid robot project *Cog*, [4]. Under such framework, oscillatory motions were integrated with a sliding modes controller for position control of the end-effector.

On previous work on neural oscillators, the parameters need to be inserted off-line, using a trial-and-error approach to estimate their value. An automatic approach operating on the frequency domain for selecting the parameters was proposed in [2], [1]. However, a time-domain analysis is required to both provide additional insight into the dynamics of the non-linear model, and as an alternative, more intuitive method to tune the parameters.

Tools and toys are often used in a manner that is composed of some repeated motion – consider hammers, bells, saws, rattles, drummers, brushes, files, etc. Therefore, strategies for the oscillatory control of movements of a humanoid robot are imperative, especially if they result on *natural* movements, which is the case of Matsuoka neural oscillators, since they track the natural frequency of the dynamic system to which they are coupled. As results in Figure 6 show, playing musical instruments is an application where tuning of oscillations plays a rather important role. The wrong set of parameters may result in no oscillations or else low-amplitude or low-frequency oscillations, which is an undesirable behavior. But using the tools described in this paper, tuning is fast and effective.
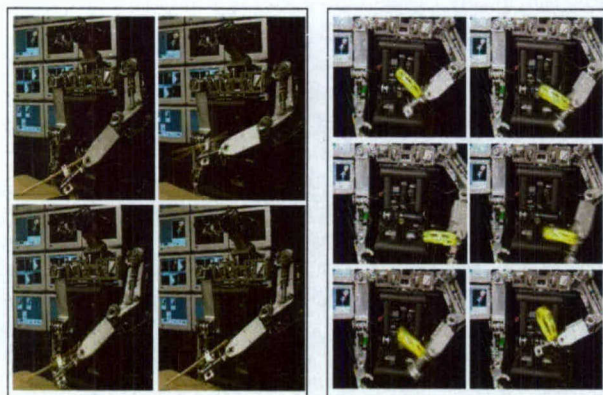

Fig. 6. The humanoid robot Cog playing two musical instruments – a drum (left) and a tamborine (right), after tuning of the neural oscillators. The robot first reaches the instrument using a Sliding Modes Controller [3].

Such production of sounds is closely associated to the neural oscillator's property of entraining the natural frequency of the dynamic system to which it is coupled. Figure 7 shows results for two different experiments consisting of having the robot shake a Castonete and a Rattle for producing musical sounds, with and without activation of joint feedback. Clear rhythmic sounds are produced with feedback. But without it the robot's arm shakes loose (no entrainment), and the rhythmic sound just does not come out.
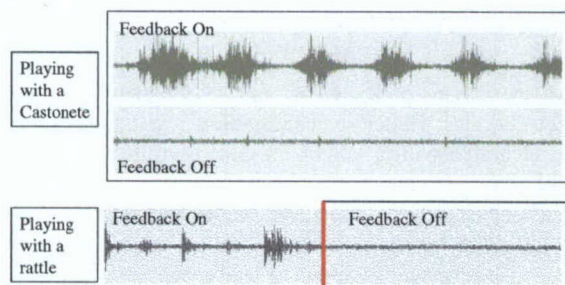

Fig. 7. Rhythmic sounds produced by having the robot play two musical instruments – a Castonete, and a rattle – with and without joint feedback. No entrainment occurs, and therefore rhythmic production of sounds is inhibited, without joint feedback.

VI. DISCUSSION AND CONCLUSIONS

Piece-wise linear analysis, Lorenz maps, contraction analysis, invariant set theory and *Poincaré* maps were used to infer stability properties of the neural oscillator. These mathematical tools were also used to bring insight to the oscillator state-space dynamics.

The oscillator dynamics was characterized in terms of its parameters. This way, the design of oscillators for control is facilitated, as well as the evaluation of transients and frequency bandwidth. This analysis provides, therefore, theoretical support for the control of robotic arms using Matsuoka neural oscillators. In addition, these oscillators are widely applied on walking robots to generate rhythmic walking patterns [11], [12], for which this analysis will be an useful design tool.

REFERENCES

[1] A. M. Arsenio, "On Stability and Error Bounds of Describing Functions for Oscillatory Control of Movements", IEEE International Conference on Intelligent Robots and Systems, 2000.
[2] A. M. Arsenio, "Neural Oscillator Networks for Rhythmic Control of Animats", From Animals to Animats 6, MIT-Press, 2000.
[3] A. M. Arsenio, "Developmental Learning on a Humanoid Robot", IEEE International Joint Conference on Neural Networks, 2004.
[4] R. A. Brooks and L. A. Stein, "Building Brains for Bodies", Autonomous Robots, 1(1):7-25, 94.
[5] J. M. Gonçalves, "Analysis of Switching Systems", PhD thesis proposal, MIT EECS department, 99.
[6] E. R. Kandel, J. H. Schwartz and T. M. Jessell, "Essentials of Neural Science and Behavior", Appleton & Lange, 95.
[7] W. Lohmiller and J-J. E. Slotine, "On Contraction Analysis for Nonlinear Systems", Automatica, 34(6), 98.
[8] K. Matsuoka, "Sustained Oscillations Generated by Mutually Inhibiting Neurons with Adaptation", Biological Cybernetics, 52:367-376, 85.
[9] J-J. E. Slotine and W. Li, "Applied Nonlinear Control", Englewood Cliffs, NJ, Prentice-Hall, 91.
[10] S. H. Strogatz, "Nonlinear Dynamics and Chaos", Addison-Wesley, 94.
[11] G. Taga, Y. Yamaguchi and H. Shimizu, "Self-organized Control of Bipedal Locomotion be Neural Oscillators in Unpredictable Environment", Biological Cybernetics, 65:147-159, 91.
[12] G. Taga, "A Model of Neuro-Musculo-Skeletal System for Human Locomotion", Biological Cybernetics, 95.
[13] M. Williamson, "Robot Arm Control: Exploiting Natural Dynamics", Ph.D. Thesis, MIT, 99.